

Central Metal Determines Pharmacokinetics of Chlorophyll-Derived Xenobiotics

Małgorzata Szczygiel,[†] Krystyna Urbańska,^{*,†} Patrycja Jurecka,[†] Iwona Stawoska,^{†,‡} Grażyna Stochel,[‡] and Leszek Fiedor^{*,†}

Faculty of Biochemistry, Biophysics and Biotechnology, Jagiellonian University, Cracow, Poland, Faculty of Chemistry, Jagiellonian University, Cracow, Poland

Received December 31, 2007

Chlorophyll derivatives are potentially dangerous xenobiotics of dietary origin. The interactions of water-soluble derivatives of chlorophyll a with the animal organism were investigated using chlorophyllide a and its Zn-substituted analogue as model xenobiotics. The chlorophyllides were administered to tumor-bearing mice and their uptake, distribution, and clearance were compared. The centrally bound metal determines important aspects of the *in vivo* behavior of metallochlorophyllides as xenobiotics. The uptake and clearance of chlorophyllide a were significantly faster than those of [Zn]-chlorophyllide a. Chlorophyllide a showed some tissue selectivity, while [Zn]-chlorophyllide a was uniformly distributed among tissues. Interestingly, the tissue levels of the latter compound were ten times higher than those of the Mg-derivative. These differences indicate that [Zn]-chlorophyllide a, in contrast to chlorophyllide a, is only weakly recognized by the system of active transport of xenobiotics and by enzymes involved in chlorophyll metabolism. The dependence of chlorophyllide pharmacokinetics on the central metal is of great relevance to chlorophyll-based phototherapy.

Introduction

Chlorophylls (Chls)^a are usually referred to as key photosynthetic pigments. Not often, however, if at all are their interactions with the animal world remarked upon.^{1–5} These are not as uncommon as it may appear. One of them, on a purely aesthetic level, relates to our visual perception of Chls as green pigments of flora. Another feature, of immediate relevance to virtually all herbivorous animals, is the continuous uptake of chlorophyllous pigments with plant-derived foods.^{4,5} Also, for their remarkable physicochemical characteristics, Chls have become increasingly under scrutiny as photosensitizing agents for photodynamic therapy (PDT).^{6–10} Chlorophylls and bacteriochlorophylls, having intense absorption in the red and NIR, respectively, and being "biocompatible", appear more advantageous than synthetic photosensitizing agents.^{11–13} For instance, palladium-substituted bacteriopheophorbide a comes out very well in the final stages of clinical trials for cancer treatment.¹³

The impact of chlorophyll-derived xenobiotics on animals and humans has only recently been appreciated, after it was shown that pheophorbide a (Pheide a), a water-soluble metabolic intermediate of Chl a, diffuses from the digestion tract to circulation and then to tissues.⁵ The presence of this highly photocytotoxic pigment in the body poses more risk to the animal than many other xenobiotics do.^{7,14} The inevitable intake of Chls (and other xenobiotics) lead in animals to the evolution of efficient protective mechanisms. Forming one line of defense, highly specialized membrane proteins, such as multidrug-resistance proteins (MDRs), capable of promoting the vectorial transport of xenobiotics across cellular membranes, are recruited in cells of various organs. For protection against porphyrins and

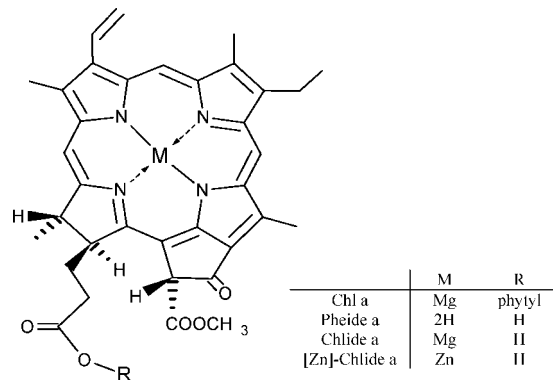


Figure 1. Chemical structures of Chl a and its water-soluble derivatives.

Chl derivatives of dietary origin, a key role has been assigned to a specific transporter known as the breast cancer resistance protein (BCRP or ABCG2).^{14,15} The activity and efficiency of this vitally important defense system, i.e., xenobiotic efflux, poses a serious therapeutic problem. In various kinds of diseases, it confers resistance to many drugs, including most anticancer chemotherapeutic agents.^{16–18} By the same token, similar difficulties can be anticipated if one intends to apply exogenous photosensitizers in PDT.^{17–19}

In the present model study, we aimed to shed more light on the molecular principles of the *in vivo* transport and clearance of xenobiotics derived from Chl a. Another goal was to determine whether the interactions of Chl derivatives with tumor *in vivo* depend on the type of the central metal. Our approach was to apply Mg- and Zn-substituted Chlides as model xenobiotics and, taking advantage of their spectroscopic features, monitor their fate and interactions within the animal organism. Both pigments, which are close structural analogues of the dietary phototoxin Pheide a (structures shown in Figure 1), are water-soluble and can with ease be tracked in tissues. Importantly, the major effect caused by central metal replacement concerns the elevated stability of the xenobiotic. Because of a strong chelation of the Zn²⁺ ion by the macrocycle, [Zn]-Chlide

* To whom correspondence should be addressed. Phone: +48-12-6646803 (K.U.); +48-12-6646358 (L.F.). Fax: +48-12-6646902 (K.U.); +48-12-6646902 (L.F.). E-mail: urbanska@mol.uj.edu.pl (K.U.); lfiedor@mol.uj.edu.pl (L.F.).

[†] Faculty of Biochemistry, Biophysics and Biotechnology, Jagiellonian University.

[‡] Faculty of Chemistry, Jagiellonian University.

^a Abbreviations: Chl: chlorophyll; Chlide: chlorophyllide; [Zn]-Chlide a: Zn²⁺-complexing chlorophyllide a; Pheide: pheophorbide; PDT: photodynamic therapy; ip, intraperitoneally.

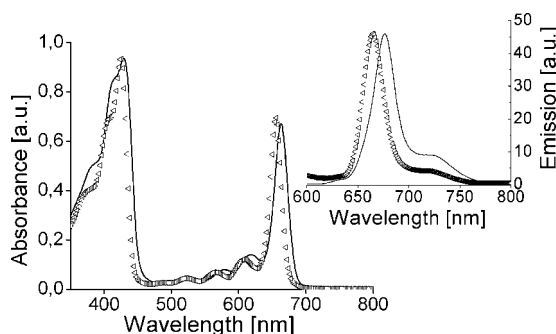


Figure 2. Electronic absorption and emission (inset) spectra of tissue (intestine) extracts obtained from the Chlide a (solid line) and [Zn]-Chlide a (dotted line) treated mice. The extractions were done using 90% aqueous acetone (see the text for details). Absorption spectra were normalized to the intensity of the Soret band. Emission spectra were measured at room temperature, applying the excitation to the maximum of the Soret band.

a is significantly less labile toward demetalation than Chlide a.^{4,20–22} The use of two different metallochlorophyllides allowed us to address important questions concerning xenobiotics originating from Chls: (i) whether the type of the centrally chelated metal ion is relevant to their *in vivo* interactions and if so to what extent, (ii) how their elimination from the body is related to chemical stability. Our results show that the central metal plays a decisive role in determining the fates of Chl-derived xenobiotics.

Results

Uptake of Xenobiotics. The xenobiotics were identified on the basis of the emission and absorption spectra (Figure 2), and their concentrations were estimated from the respective calibration curves. The distribution of intraperitoneally administered Chlide a and [Zn]-Chlide a in mice tissues is shown on the chart in Figure 3 (the results of tissue analysis are listed in Table S1 in the Supporting Information). Almost all tissues showed a rapid uptake of Chlide a, maximal levels of this compound being reached within 0.5 h, the earliest experimental time point. A slower uptake of Chlide a occurred with blood (peak at 4 h), eyes, and tumor (both peak at 10 h).

The kinetics of [Zn]-Chlide a uptake were generally much slower, and a rapid uptake was observed only in the case of skin (peak time 0.5 h). In blood, liver, and eyes, the peak levels of [Zn]-Chlide a were reached at 4 h and in other tissues at 10 h after injection.

Clearance of Xenobiotics. Chlide a was rapidly eliminated from the body, and in most cases, the Chlide a clearance profile could be described by a monoexponential decay with a half-life $\tau_{1/2}$ of about 13.5 h (Table 1). Within 48 h after ip injection, nearly 100% of xenobiotic was cleared out, and after that time, only weak signals of the xenobiotic, close to a background level ($\leq 1.5 \times 10^{-7}$ g/g, intrinsic fluorophores), were detected in most tissues. Only in liver, spleen, and intestine were slightly higher levels found ($\sim 3–4 \times 10^{-7}$ g/g).

The elimination of [Zn]-Chlide a was significantly slower, and after 4 h and longer intervals, its tissue levels were by 1 order of magnitude higher (except in the intestine) than the corresponding levels of Chlide a. These high levels of [Zn]-Chlide a were maintained up to 72 h after injection and only then did a slow decrease occur. At the end of the experiment (120 h), the xenobiotic content in most tissues still considerably exceeded a background level, indicating that the *in vivo* lifetime of this compound is longer than the time span of the experiment.

The elimination profile of [Zn]-Chlide a could be approximated as an almost linear process with a $\tau_{1/2}$ value of about 44 h (Table 1).

Tissue Levels. The maximal Chlide a content was detected in intestine (23.7×10^{-7} g/g) and in liver (17.5×10^{-7} g/g), being in both cases significantly higher than in blood at any time (max 6.6×10^{-7} g/g). A relatively high concentration of Chlide a was detected in skin and muscles ($\sim 8 \times 10^{-7}$ g/g), while in the remaining tissues, a much lower content of this xenobiotic, between 1 to 5×10^{-7} g/g, was found.

The distribution of [Zn]-Chlide a followed a different pattern (Figure 3). A very high level of [Zn]-Chlide a, between 33 and 26×10^{-7} g/g, was maintained in blood for a long period (up to 72 h past injection). A comparably high content of this xenobiotic was found only at peak times in the reticuloendothelial cell-containing organs, i.e., liver (32.5×10^{-7} g/g at 4 h) and spleen (24.1×10^{-7} g/g at 10 h). In other tissues (heart, lungs, kidneys, and skin), a slightly lower level, from 14 to 24×10^{-7} g/g, was detected up to 24 h. The lowest concentrations of [Zn]-Chlide a ($> 13 \times 10^{-7}$ g/g) were at all time points found in eyes, muscles, and intestine; in these tissues, the xenobiotic content reached a background level after 96 h.

Content in Tumor. Table 2 lists the relative ratios of the tumor-to-overlying-muscle (*T/M*) contents for the two Chlides at different time points. In the case of Chlide a, a satisfactory value of the *T/M* ratio (2.4 and 4.7) was achieved only after 24 and 72 h, but the xenobiotic concentration in the tumor was rather low (up to 1.1×10^{-7} g/g). By contrast, the level of [Zn]-Chlide a within 10 h reached as much as seven times higher values (6 to 9×10^{-7} g/g) and stayed high until the end of the experiment. Also, an advantageous value of the *T/M* ratio for [Zn]-Chlide a, ranging from 2.5 to 7.5, was observed for a very long period at 48, 72, and 96 h after administration. This indicates a slower clearance of [Zn]-Chlide a from the tumor than from the overlying tissue.

Mass Balance. To determine the amounts of xenobiotic that accumulated in the tissues, partial mass balances throughout the experimental time points were estimated (Figure 4A), defined as the ratio of total amount of xenobiotic found in all analyzed tissue to the amount injected, without taking into account excreted material, which was analyzed in a separate experiment (see below). The highest recovery of [Zn]-Chlide a, as much as 20% of the initial dose, was obtained within 10 h after the treatment. The highest recovery of Chlide a, at the earliest time point measured, was only 5%. At the end of the experiment (120 h) the recovery of [Zn]-Chlide a still amounted to as much as 1.3% of the injected dose, whereas the amounts of recovered Chlide a did not exceed a background level already after 48 h.

The results of the noninvasive monitoring of xenobiotics' excretion in feces from mice housed in metabolic cages are shown in Figure 4B. The summation of the xenobiotic amounts detected enabled an estimate of the (cumulative) recovery of the excreted intact pigments, which by the end of the experiment amounted to 2% of the administered Chlide a and 6% of [Zn]-Chlide a; no Pheide a was detected in feces. The highest levels ($\sim 0.22 \mu\text{g/g}$) of nonmetabolized [Zn]-Chlide a in feces were detected between 1.5 and 4 h, and then its content dropped to a background level. The monitoring of Chlide a did not show any significant increase in its level in feces throughout the experiment, and the simultaneous analysis of urine samples showed no traces of intact xenobiotics (results not shown).

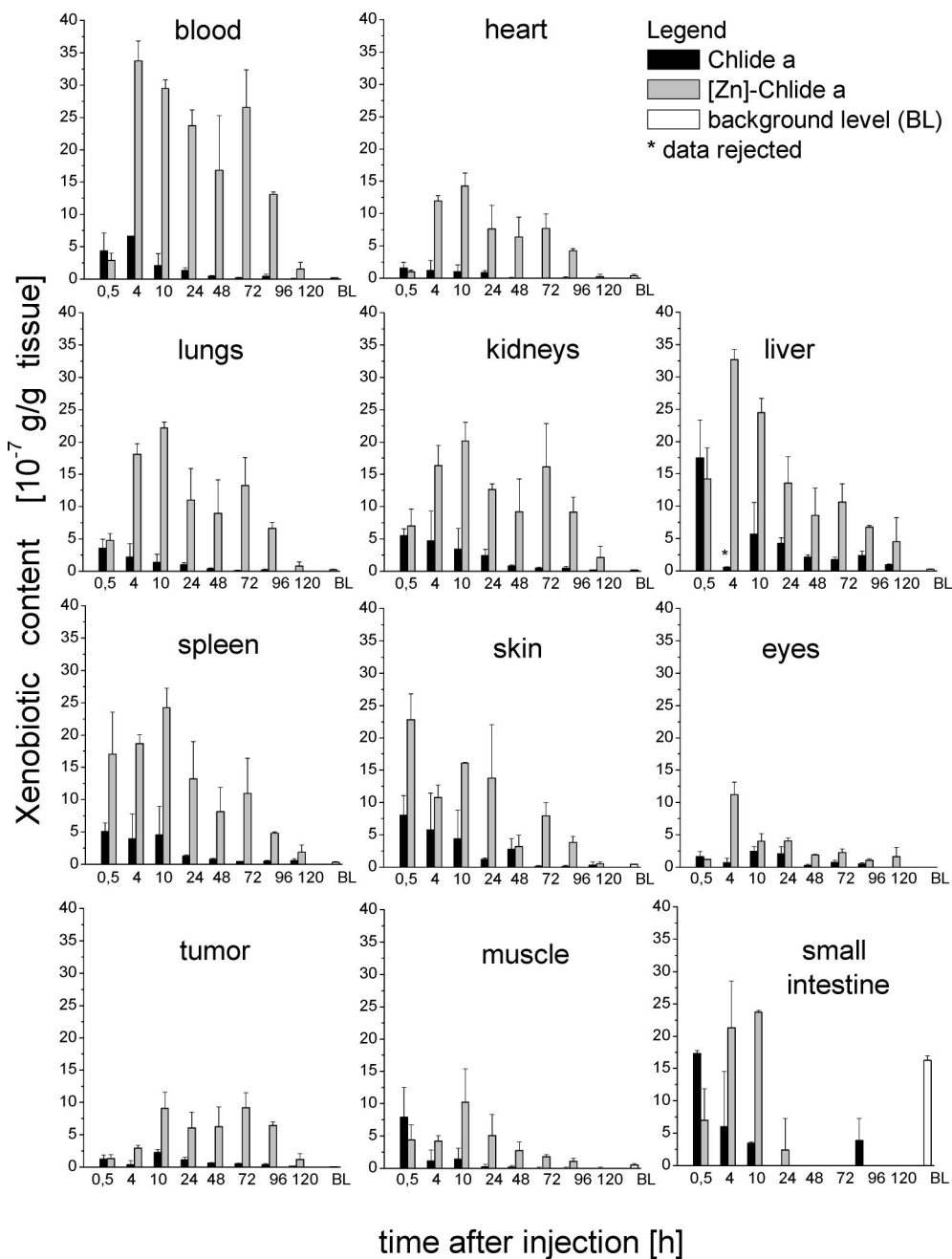


Figure 3. Distribution of Chlide a and [Zn]-Chlide a in tissues of DBA/2 mouse at various times after administration. The xenobiotics (as PBS solution) were injected intraperitoneally into the animals. The charts show mean values determined in independent analysis of samples taken from 2–4 animals (see the text for details). The background level (BL) denotes the content of Pheide a in tissues of untreated animals. The values of standard errors are also indicated.

Aggregation in Aqueous Media. The two derivatives of Chl a used as model xenobiotics are well soluble in organic solvents and the removal of the phytol and presence of the free carboxylic group markedly increases their solubility in aqueous media.^{23,24} Nevertheless, their solubility in water is quite limited and aggregation may influence their mobility in tissues. Because aggregation leads to a very efficient quenching of Chl emission,²⁵ measurements of the dependence of fluorescence intensity on concentration were applied to monitor the formation of the aggregates. As shown in Figure 5, the concentration effect is sharper in the case of [Zn]-Chlide a, indicating that its aggregation occurs already at quite low concentrations ($\sim 1 \mu\text{g/mL}$). The quenching of Chlide a emission occurs only at higher

concentrations and the pigment stays in a monomeric form up to the concentration of $7\text{--}8 \mu\text{g/mL}$.

Discussion

The objective of the present work was to evaluate to what extent the interactions of chlorophyll-derived xenobiotics within the animal body, in particular their tissue distribution and retention, are determined by the chemical stability and the type of the central metal. Both metallochlorophyllides used in the present study as model xenobiotics are relatively well water-soluble derivatives of a natural plant pigment, Chl a, and its dietary metabolite, Pheide a, and they differ only by the occupant of the central cavity. Because the central metal ion is well shielded (in plane) by the chelating macrocycle, the structural

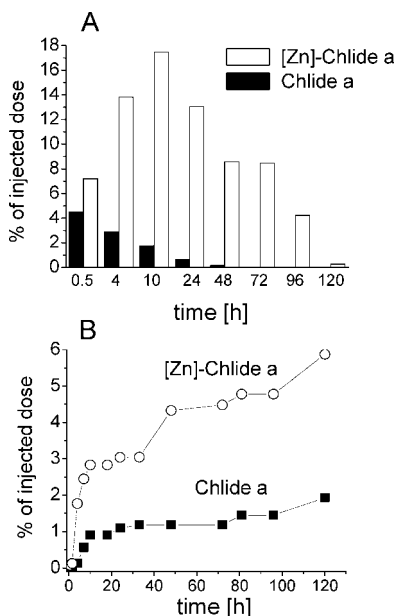
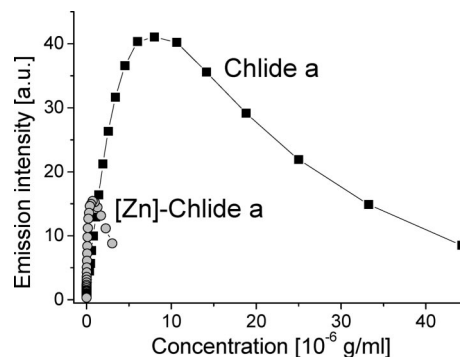
Table 1. Peak Times and “Half-Lifetimes” of Chlide a and [Zn]-Chlide a after ip Administration in DBA/2 Melanoma Tumor Bearing Mice

organs	Chlide a		[Zn]-Chlide a	
	peak [h]	$\tau_{1/2}$ [h]	peak [h]	$\tau_{1/2}$ [h]
blood	4	4	4	73
heart	0.5	23	10	48
lungs	0.5	12	10	50
kidneys	0.5	22	10	78
liver	0.5	7	4	27
spleen	0.5	10	10	38
skin	0.5	24	0.5	44
eyes	10	24	4	27
tumor	10	17	10–72	28
muscles	0.5	2	10	24
intestine	0.5	3	4–10	
mean value \pm SE				
	2.55 \pm 1.15	13.45 \pm 2.67	10.00 \pm 3.22	44.00 \pm 6.07

Table 2. Tumor-to-Overlying-Muscle (T/M) Tissue Ratio for Chlide a and [Zn]-Chlide a after ip Administration in DBA/2 Melanoma Tumor Bearing Mice

tissue ratio	Chlide a	[Zn]-Chlide a
0.5 h	0.16	0.31
4 h	0.49	0.74
10 h	1.32	0.90
24 h	2.41	1.07
48 h	1.43	2.54
72 h	4.96	5.84
96 h		7.45

differences between the model xenobiotic are insignificant. However, metal replacement may cause several effects of potential relevance for in vivo interactions: (i) a stronger chelation of the Zn ion by the Chl macrocycle greatly enhances its stability, and [Zn]-Chlide a is more resistant to demetalation than Chlide a, (ii) the coordinative properties of the two Chlides are somewhat different as the central Zn^{2+} binds preferentially one or no axial ligand while the central Mg^{2+} ion readily accepts

**Figure 4.** (A) Comparison of partial (without considering feces) mass balances of ip injected Chlide a and [Zn]-Chlide a into mice. The values shown were corrected for the control level. (B) Comparison of cumulative recoveries of Chlide a and [Zn]-Chlide a in feces collected from mice kept in metabolic cages. Feces samples were collected in various intervals up to 120 h after administration.**Figure 5.** Dependence of emission (fluorescence) intensity on the concentration of Chlide a and [Zn]-Chlide a in PBS solution.

(and strongly binds) two axial ligands,²⁶ and (iii) differences in the coordination of ligands to the central metal may affect aggregative properties of xenobiotics.

Animal Model. DBA mice bearing the Cloudman S91 melanoma used in the present study is a convenient model tumor, routinely used in our laboratory in studies of various approaches to cancer therapy, including photodynamic therapy.^{27–31} The mice weigh about 25 g each, which is less than other laboratory animals, e.g., hamsters (100–120 g), and hence smaller amounts of photosensitizers are required. Most importantly, the tumor S91 cells can be cultured in vitro and after a subcutaneous inoculation induce tumors practically in 100% of cases. The tumors grow exponentially and display only a little size scatter between animals.

Uptake and Clearance of Xenobiotics. Both the uptake and clearance of Chlide a from mice were much quicker than those of [Zn]-Chlide a. In most tissues, maximum levels of Chlide a were reached during the first 30 min while [Zn]-Chlide a peaks after 4–10 h following ip treatment. This fast rise indicates that both xenobiotics are relatively rapidly distributed from the ip space. The initial rise of xenobiotic level in the tissues obviously reflects the build up of xenobiotic content in tissues via a diffusion driven by a high concentration gradient. The 4–10 h lag in the rise in tissues levels of [Zn]-Chlide a can be attributed to a slower diffusion of this xenobiotic through tissues, caused by its aggregation. The higher tendency of [Zn]-Chlide a to form aggregates in an aqueous environment is confirmed by a strong quenching of fluorescence, which occurs even at low concentrations. This is in agreement with the role of the central metal in the aggregation of Chls shown in previous studies.^{24,32,33} However, the kinetics of xenobiotic uptake seem not to be entirely diffusion-controlled, and several indications point to the involvement of active transport system (see below). Main arguments for the active transport are a very fast (0.5 h) appearance of intact xenobiotics in the small intestine and liver, where their levels rise quicker than in the circulation and other tissues.

The two Chlides show even greater differences in their clearance as Chlide a is completely cleared from the body within 24 h, while significant levels of [Zn]-Chlide a are still detected after 120 h. Surprisingly, in spite of the presence of a considerably high (secondary) gradient of [Zn]-Chlide a concentration in the body, there is no diffusion of the xenobiotic into the intestine.

The analysis of xenobiotic content in feces collected from the xenobiotic-treated mice kept in metabolic cages also reveals differences between [Zn]-Chlide a and Chlide a. Regardless of the level of Chlide a in the small intestine, only trace amounts of Chlide a, close to a background level, were detected in feces.

In contrast, significant quantities of [Zn]-Chlide a could be detected in feces but only when it was also found in the small intestine. The absence of Chlide a outside the small intestine is most likely due to the action of intestinal microflora, located mainly in the large intestine and known to contribute to the metabolism of various xenobiotics under anaerobic conditions.^{34,35} This degradation pathway is seemingly less effective in the case of [Zn]-Chlide a.

Tissue Distribution and Mass Balance. The type of central metal in the Chl-derived xenobiotic has a large effect on both the tissue levels and the recovery of the xenobiotic and seems to only weakly influence the pattern of its distribution in tissues. [Zn]-Chlide a was found to be more or less uniformly distributed among tissues while there is some tissue selectivity (liver, intestine) toward Chlide a. Furthermore, the two xenobiotics reveal substantial differences in their levels in tissue, which become apparent as early as 0.5 h after administration (peak time for Chlide a) and which increase over longer periods. In the extreme case, the levels of [Zn]-Chlide a exceed by at least 10-fold the levels of Chlide a.

The large differences between Chlide a and [Zn]-Chlide a in their *in vivo* fate are evident from an estimation of mass balance. The recovery of Chlide a (~6.5%) is very low compared to that of [Zn]-Chlide a (~24%). These differences indicate that a major part of the administered Chlide a undergoes a quick metabolic degradation to nonfluorescent products, while the metabolism of [Zn]-Chlide a is much slower. The slow rate of the latter metabolism can be related to an increase in its chemical stability due to the strong chelation of the Zn²⁺ ion by the tetrapyrrole. The pathways of Pheide a/Chlide a biodegradation in animals remain unknown but, by analogy, they are likely to follow that of heme degradation. A crucial step in this process, catalyzed by heme oxygenase, is the cleavage of the macrocycle and the release of ferric ion. The resultant biliverdin IX α is then converted to bilirubin by a specific reductase, followed by a microbial conversion of this intermediate in the large intestine to final products excreted with feces. Apparently, the metabolic breakdown of Chlide a is quick because its macrocycle is labile; the strongly stabilized Zn complex is less susceptible to the enzymatic degradation. A similarly slow degradation was observed with zinc porphyrin, which is produced instead of heme under conditions of iron deficiency and which cannot be metabolized, thereby being deposited in the spleen and liver.³⁶

Involvement of Active Transport. Because of a very close structural similarity to Pheide a, it seems reasonable to assume that Chlide trafficking occurs at least partially actively and that, consequently, BCRP might also be involved in this transport. There are several indications to support this notion: the liver and intestine, regarded as tissues of high BCRP activity,^{16,37,38} show a fast accumulation of Chlide a, in line with a previous pharmacokinetic study on derivatives of Chl a.³⁹ Also, Pd-substituted bacteriopheophorbide a showed an extremely short (below 1 h) lifetime in mice.⁴⁰ These findings point to the involvement of an active transport in the efflux of these xenobiotics, which parallels their metabolic processing. Intriguingly, in the case of [Zn]-Chlide a, while this pathway of active transport does not seem to be very effective, it is not entirely clear what alternative explanation there may be for the sudden drop in the rate of [Zn]-Chlide a efflux in longer periods after its administration. As shown above, the intact [Zn]-Chlide a can hardly be detected in the intestine and in feces (after the peak time), despite the fact that still very high levels of the xenobiotic are present in most tissues and its retention time is

much longer than that of Chlide a. These differences in the pharmacokinetics of Chlide a and [Zn]-Chlide a point to some substrate specificity of the active transport and imply that Zn-substituted Chlide cannot be recognized by the transport system. However, this finding remains somewhat surprising, first because BCRP shows a relatively low substrate specificity^{16,18} and, second, it seems difficult to suggest a plausible molecular basis for such a difference between such closely related substrates.

Relevance to Photodynamic Therapy. Photodynamic therapy relies on the use of two components, light and a photosensitizer (pro-drug), which on their own show no or very little cytotoxicity. A major advantage of PDT stems from the selective application of light to locally activate the photosensitizer and enable the eradication of malignant tissue with negligible damaging effects to healthy tissue. An optimal timing for the treatment is the point when the photosensitizer concentration and the *T/M* ratio are maximal.⁴¹ The tumor tissue shows only a moderately preferential uptake of both model xenobiotics, but the levels and the *T/M* ratio (~5.3) of [Zn]-Chlide a are much higher than those of Chlide a. For this reason, [Zn]-Chlide a is potentially a much better tumor localizer than Chlide a, rendering it very promising for the PDT treatment of cancer. Moreover, the increased level of the pigment in tumor tissue may allow for reduction of the administered doses. Furthermore, the retention time of the Zn complex in malignant tissue is long enough (half-life $\tau_{1/2} \approx 44$ h) to allow a multiple application of irradiation following a single administration. On the other hand, the retention time of [Zn]-Chlide a is still considerably shorter than the retention time of commercially available hematoporphyrin derivative.⁴² This is very promising in terms of minimizing the dangerous side effects of cutaneous phototoxicity. However, it is not obvious how pharmacokinetic behavior of photosensitizer translates into the photodynamic activity *in vivo* and thus the correlation between efficacy in tumor eradication and retention/distribution of photosensitizer requires experimental confirmation.

Conclusions

The present studies show that the type of central metal greatly influences the *in vivo* fate of Chl-derived xenobiotics and provide a guideline for modifications of Chl/porphyrin-based photosensitizers, but their relevance extends beyond applications in PDT. The substitution of the central metal by a heavier divalent metal ion affects not only physicochemical parameters of Chl-derived photosensitizers but also their pharmacokinetics. The uptake and clearance of ip administered Chlide a is very quick, whereas [Zn]-Chlide a shows much slower kinetics; the tissue distributions of both xenobiotics also show a different pattern. In the case of [Zn]-Chlide a, there was no preferential accumulation and the pigment was more or less uniformly distributed among animal tissues, whereas Chlide a shows a somewhat higher affinity toward the liver and intestine. The two metallochlorophyllides show very different rates of metabolic degradation, most likely related to the elevated chemical stability of the Zn complex. If the active transport is also involved in the elimination of chlorophyllides, our results indicate that it can be circumvented by a simple substitution of Mg for Zn. This central-metal-controllable retention time of metallochlorophyllides *in vivo* may render them more favorable than the photosensitizers already earmarked for clinical use.

Experimental Section

Preparation of Model Xenobiotics. Chl a was extracted from cyanobacterium *Spirulina laporte*, obtained from the Culture

Collection of Autotrophic Organisms in Trebon (Czech Republic). The pigment was purified by column chromatography on DEAE-Sepharose CL-6B (Pharmacia), pre-equilibrated in acetone.⁴³ The elution of Chl a was done with 15% MeOH in acetone (v/v).

Chlide a was prepared from Chl a via enzymatic removal of phytol, a C₂₀ alcohol esterifying the C-17 propionic acid side chain (Figure 1), using plant enzyme chlorophyllase (EC number 3.1.1.14) isolated from leaves of *Fraxinus excelsior*, according to a previously described procedure.^{24,44} Briefly, the enzyme was reconstituted from the acetone powder by solubilization with 1% Triton X-100 in 0.1 M phosphate buffer (pH 7.6). The reconstituted enzyme was then used to catalyze hydrolysis of Chl a. The reaction was initiated by adding small volume of acetone solution of Chl a to the reconstituted enzyme. After 5–6 h of vigorous stirring at 37 °C under Ar, the reaction mixture was extracted with diethyl ether. The product was purified by column chromatography on CM-Sepharose CL-6B (Pharmacia).⁴⁴ Pheophorbide a (Pheide a) was obtained from Chlide a via demetalation with glacial acetic acid and then purified on CM-Sepharose CL-6B as above. [Zn]-Chlide a was obtained from Pheide a via direct metalation with zinc acetate in methanol.²² After the completion of the reaction, the solvent was removed under vacuum and the residue was dissolved in a small volume of glacial acetic acid. The product, [Zn]-Chlide a, was purified twice on CM-Sepharose CL-6B. The model xenobiotics were prepared in several independent batches. All pigment preparations and their handling were performed as quickly as possible and under dim light to avoid degradation. Under proper conditions (dryness, −40 °C, Ar atmosphere), purified Chlides can be stored for several weeks without traces of degradation, but we made sure that always freshly prepared and nondegraded compounds were injected into animals. The xenobiotics were thoroughly purified, and before each pharmacokinetic experiment, the sample integrity was confirmed spectrophotometrically and chromatographically whenever necessary.

To compare the ability of the two xenobiotics to form aggregates in aqueous media, a series of their solutions in the phosphate buffered saline (PBS) was prepared and the intensity of the emission was measured as a function of concentration. The solutions were excited at 414 nm (Chlide a) or at 410 nm ([Zn]-Chlide a) and their fluorescence spectra were recorded within a range between 600 and 850 nm. The spectra were measured in 1 cm quartz cells at ambient temperature by using an LS 50 Perkin-Elmer fluorometer (Beaconsfield, UK).

Tumor and Animal Model. S91 Cloudman mouse melanoma cell line was derived from PC1A clone obtained from the American Type Culture Collection. The cells were grown as monolayers at 37 °C in a humidified atmosphere containing 5% CO₂ in the RPMI medium, containing 5% fetal calf serum and supplemented with antibiotics (penicillin and streptomycin), as described by Cieszka et al.^{27,28} Just before tumor inoculation, cells were washed with warm PBS and harvested by trypsinization. The cell suspension was centrifuged, the pellet (~1 × 10⁶ cells) was washed with PBS, taken up in 0.1 mL PBS, and implanted subcutaneously into the right thighs of DBA/2 mice. The tumors grew visible ten days after implantation. The tumor volumes were estimated on the basis of their three perpendicular diameters.^{45,46} The mean diameter *d* of the tumor was calculated according to the expression $d = (a \times b \times c)^{1/3}$, where *a*, *b*, and *c* stand for the respective diameters of the tumor.

Male DBA/2 mice, bearing the Cloudman S91 melanoma, were used in the present study. The mice were 3–4 months old and about 25 g each. The animals were treated with the xenobiotics when the *d* parameter reached 1.5 cm. The animals used in the present study were obtained from the animal breeding facility at the Faculty of Biochemistry, Biophysics, and Biotechnology, Jagiellonian University, Cracow. The mice were kept on a standard laboratory diet with free access to drinking water. The use of the animals for experimental purposes was approved by the Jagiellonian University Committee for Ethics of Experiments on Animals (permission no. 39/2006).

Experimental Groups. The mice were divided into the following experimental groups: (1) Melanoma-bearing mice treated with

Chlide a. The tissue samples were taken after 0.5, 4, 10, 24, 48, 72, 96, and 120 h following pigment administration. At each time point, 2–4 mice were analyzed. (2) Melanoma-bearing mice treated with [Zn]-Chlide a. The tissue samples were taken at the same time points as above. At each time point, 2–4 mice were analyzed. Group (3) was the control group. Tissue samples were taken from two untreated melanoma-bearing mice. Altogether, 48 mice were used in the experiment.

In another experiment, a group of male DBA/2 mice bearing the S91 melanoma tumor were housed in metabolic cages (Tecniplast, Italy) and treated with xenobiotics when the *d* parameter reached 1.5 cm. Urine and feces were collected from the animals over the following intervals after treatment: 0–0.5, 0.5–1.5, 1.5–4, 4–7, 7–10, 10–18, 18–24, 24–33, 33–48, 48–72, 72–81, 81–96, and 96–120 h. The samples were stored at −30 °C pending analysis.

Administration of Xenobiotics. A portion of a dried pigment, in a dose of 10 mg per 1 kg body weight, was taken up in a small volume (60–100 μL) of ethanol, placed in a test tube, diluted with 2 mL of PBS, and sonicated for 3 min. The solution was centrifuged at 2000g for 10 min at room temperature in order to remove any insoluble material. The supernatant was immediately injected intraperitoneally (ip) into the animals. Because of precipitation, the actual injected doses of the xenobiotics per single animal were 0.19 mg for Chlide a and 0.15 mg for [Zn]-Chlide a.

Analysis of Xenobiotic Distribution. The animals were anesthetized using Morbital (Biowet, Poland), and their organs and tissue samples were excised, weighed, and then stored at −30 °C until further analysis. The content of Chl derivatives in the tissue samples was analyzed fluorometrically according to a previously described method with slight modifications.³⁹ Briefly, in order to extract the xenobiotics, tissue samples, weighing from 0.05 to 1.3 g, were homogenized for 1 min in 7 mL of ice-cold 90% aqueous acetone using a tissue homogenizer MPW-120 (Medical Instruments, Poland). The homogenate was centrifuged at 2000g for 10 min at 4 °C, the supernatant collected, and the pellet re-extracted with 7 mL of 90% aqueous acetone to ensure a complete recovery of the pigment. The extracts were pooled and analyzed for pigment content. The samples were excited at 414 nm (Chlide a) or at 410 nm ([Zn]-Chlide a), and their fluorescence spectra were recorded in the range between 600 and 800 nm. A comparison of the results obtained in two independent analyses of xenobiotic content in mouse tissues is shown in Figure S1 in Supporting Information.

The reliability of the analytical method was evaluated by comparing the results of pigment determination in 25 livers (the largest organ collected), each divided into two separately analyzed samples. The typical error of xenobiotic content was 3–4%, while the largest deviation from the mean value was 14%.

HPLC Analysis, Electronic Absorption, and Emission Measurements. The absorption spectra were measured on a Cary 400 spectrophotometer (Varian, USA) in 1 cm quartz cuvettes at ambient temperature. The emission spectra were measured using an LS 50 Perkin-Elmer fluorometer in a 1 cm quartz cuvette at ambient temperature. HPLC analysis (shown in the Supporting Information) was done on a reverse phase silica gel column LiChrospher 100, 4 mm × 250 mm, pore size 5 μm (Merck, Germany), using a Star 800 instrument (Varian), equipped with a TIDAS diode-array detector for online measurements of absorption spectra.

Acknowledgment. This work was supported by grants R05 043 03 (to K.U., G.S., and L.F.), N301 092 31/2881 (to K.U.), and PB 1505/P01/2007/32 (to L.F.), from the Polish Ministry of Science and Higher Education.

Supporting Information Available: Tissue levels of Chlide a and [Zn]-Chlide a. This material is available free of charge via the Internet at <http://pubs.acs.org>.

References

- Scheer, H. *Chlorophylls*; CRC Press: Boca Raton, 1991.
- Ma, L.; Dolphin, D. The metabolites of dietary chlorophylls. *Photochemistry* **1999**, *50*, 195–202.
- Grimm, B.; Porra, R. J.; Rüdiger, W.; Scheer, H. *Chlorophylls and bacteriochlorophylls*; Springer: Dordrecht, 2006; Vol. 25.
- Küpper, H.; Küpper, F. C.; Spiller, M. [Heavy metal]-chlorophylls formed in vivo during metal stress and degradation products formed during digestion, extraction and storage of plant material. In *Chlorophylls and Bacteriochlorophylls*; Grimm, B., Porra, R. J., Rüdiger, W., Scheer, H., Eds.; Springer: Dordrecht, 2006; Vol. 25, pp 67–77.
- Ferruzzi, M. G.; Blakeslee, J. Digestion, absorption, and cancer preventive activity of dietary chlorophyll derivatives. *Nutr. Res. (N.Y.)* **2007**, *27*, 1–12.
- Kessel, D.; Smith, K. M. Photosensitization with derivatives of chlorophyll. *Photochem. Photobiol.* **1989**, *49*, 157–160.
- Spikes, J. D.; Bommer, J. C. Chlorophyll and related pigments as photosensitizers in biology and medicine. In *Chlorophylls*; Scheer, H., Ed.; CRC Press: Boca Raton, 1991; pp 1181–1204.
- Henderson, B. W.; Sumlin, A. B.; Owczarczak, B. L.; Dougherty, T. J. Bacteriochlorophyll-a as photosensitizer for photodynamic treatment of transplantable murine tumors. *J. Photochem. Photobiol.* **1991**, *10*, 303–313.
- Kessel, D.; Smith, K. M.; Pandey, R. K.; Shiao, F.-Y.; Henderson, B. Photosensitization with bacteriochlorins. *Photochem. Photobiol.* **1993**, *58*, 200–203.
- Brandis, A. S.; Salomon, Y.; Scherz, A. Chlorophyll sensitizers in photodynamic therapy. In *Chlorophylls and Bacteriochlorophylls: Biochemistry, Biophysics, Functions and Applications*; Grimm, B., Porra, R. J., Rüdiger, W., Scheer, H., Eds.; Springer: Dordrecht, 2006; Vol. 25, pp 461–483.
- Rosenbach-Belkin, V.; Chen, L.; Fiedor, L.; Salomon, Y.; Scherz, A. Chlorophyll and bacteriochlorophyll derivatives as photodynamic agents. In *Photodynamic Tumor Therapy. 2nd and 3rd Generation Photosensitizers*; Moser, J. G., Ed.; Harwood Academic Publishers: Amsterdam, 1998; pp 117–125.
- Bonnett, R. Metal complexes for photodynamic therapy. In *Comprehensive Coordination Chemistry*; McCleverty, J. A., Meyer, T. J., Eds.; Elsevier: Amsterdam, 2003; pp 945–1003.
- Koudinova, N. V.; Pithus, J. H.; Brandis, A.; Brenner, O.; Bendel, P.; Ramon, J.; Eshhar, Z.; Scherz, A.; Salomon, Y. Photodynamic therapy with Pd-bacteriopheophorbide (Tookad): successful in vivo treatment of human prostatic small cell carcinoma xenographs. *Int. J. Cancer* **2003**, *104*, 782–789.
- Jonker, J. W.; Buitelaar, M.; Wagenaar, E.; van der Valk, M. A.; Scheffer, G. L.; Schepers, R. J.; Plösch, T.; Kuipers, F.; Elferink, R. P. J. O.; Rosing, H.; Beijnen, J. H.; Schinkel, A. H. The breast cancer resistance protein protects against a major chlorophyll-derived dietary phototoxin and protoporphyrin. *Proc. Natl. Acad. Sci. U.S.A.* **2002**, *99*, 15649–15654.
- Robey, R. W.; Steadman, K.; Polgar, O.; Morisaki, K.; Blayney, M.; Mistry, P.; Bates, S. E. Pheophorbide a is a specific probe for ABCG2 function and inhibition. *Cancer Res.* **2004**, *64*, 1242–1246.
- Doyle, L. A.; Ross, D. D. Multidrug resistance mediated by the breast cancer resistance protein BCRP (ABCG2). *Oncogene* **2003**, *22*, 7340–7358.
- Szakacs, G.; Paterson, J. K.; Ludwig, J. A.; Booth-Genthe, C.; Gottesman, M. M. Targeting multidrug resistance in cancer. *Nat. Drug Discovery* **2006**, *5*, 219–234.
- Higgins, C. F. Multiple molecular mechanisms for multidrug resistance transporters. *Nature* **2007**, *446*, 749–757.
- Robey, R. W.; Steadman, K.; Polgar, O.; Bates, S. E. ABCG2-mediated transport of photosensitizers. *Cancer Biol. Ther.* **2005**, *4*, 187–194.
- Schunck, E.; Marchlewski, L. Zur Chemie des Chlorophylls. *Lieb. Ann. Chem.* **1894**, *278*, 329–345.
- Watanabe, T.; Kobayashi, M. Electrochemistry of chlorophylls. In *Chlorophylls*; Scheer, H., Ed.; CRC Press: Boca Raton, 1991; pp 287–315.
- Drzewiecka-Matuszek, A.; Skalna, A.; Karocki, A.; Stochel, G.; Fiedor, L. Effects of heavy central metal on the ground and excited states of chlorophyll. *J. Biol. Inorg. Chem.* **2005**, *10*, 453–462.
- Fiedor, L.; Rosenbach-Belkin, V.; Sai, M.; Scherz, A. Preparation of tetrapyrrole–amino acid covalent complexes. *Plant Physiol. Biochem.* **1996**, *34*, 393–398.
- Fiedor, L.; Stasiek, M.; Mysliwa-Kurdziel, B.; Strzalka, K. Phytol as one of the determinants of chlorophyll interactions in solution. *Photosynth. Res.* **2003**, *78*, 47–57.
- Beddard, G. S.; Porter, G. Concentration quenching in chlorophyll. *Nature* **1976**, *260*, 366–367.
- Hartwich, G.; Fiedor, L.; Simonin, I.; Cmiel, E.; Schäfer, W.; Noy, D.; Scherz, A.; Scheer, H. Metal-Substituted Bacteriochlorophylls. I. Preparation and Influence of Metal and Coordination on Spectra. *J. Am. Chem. Soc.* **1998**, *120*, 3675–3683.
- Cieszka, K.; Hill, H.; Hill, J.; Plonka, P. Growth and pigmentation in genetically related Cloudman S91 melanoma cell lines treated with 3-isobutyl-1-methyl-xanthine and β -malanocyte-stimulating hormone. *Exp. Dermatol.* **1995**, *4*, 192–198.
- Cieszka, K.; Hill, H. Z.; Xin, P.; Azure, M.; Hill, G. J.; Boissy, R. E.; Mitchell, D. L. Survival of Cloudman mouse melanoma cells after irradiation by solar wavelengths of light. *Pigment Cell Res.* **1997**, *10*, 193–200.
- Drzewiecka, A.; Urbanska, K.; Matuszak, Z.; Pineiro, M.; Arnaut, L.; Habdas, J.; Ratuszna, A.; Stochel, G. Tritolylporphyrin dimer as a new potent hydrophobic sensitizer for photodynamic therapy of melanoma. *Acta Biochem. Pol.* **2001**, *48*, 277–282.
- Urbanska, K.; Romanowska-Dixon, B.; Matuszak, Z.; Oszajca, J.; Nowak-Sliwinska, P.; Stochel, G. Indocyanine green as a prospective sensitizer for photodynamic therapy of melanomas. *Acta Biochem. Pol.* **2002**, *49*, 387–391.
- Brindell, M.; Kulis, E.; Elmroth, S. K. C.; Urbanska, K.; Stochel, G. Light-induced anticancer activity of $[\text{RuCl}_2(\text{DMSO})_4]$ complexes. *J. Med. Chem.* **2005**, *48*, 7298–7304.
- Boucher, L. J.; Katz, J. J. Aggregation of metallochlorophylls. *J. Am. Chem. Soc.* **1967**, *89*, 4703–4708.
- Katz, J. J.; Shipman, L. L.; Cotton, T. M.; Janson, T. J. Chlorophyll aggregation: coordination interactions in chlorophyll monomers, dimers, and oligomers. In *The Porphyrins*; Dolphin, D., Ed.; Academic Press: New York, 1978; Vol. 5, pp 401–458.
- Beukveld, G.; Woithers, B.; van Saene, J.; de Haan, T.; de Ruyter-Buitenhuis, L.; van Saene, R. Patterns of Porphyrin Excretion in Feces as Determined by Liquid Chromatography: Reference Values and the Effect of Flora Suppression. *Clin. Chem.* **1987**, *33*, 2164–2170.
- Collinder, E.; Björnhag, G.; Cardona, M.; Norin, E.; Rehbinder, C.; Midtvedt, T. Gastrointestinal Host–Microbial Interactions in Mammals and Fish: Comparative Studies in Man, Mice, Rats, Pigs, Horses, Cows, Elk, Reindeer, Salmon and Cod. *Microb. Ecol. Health Dis.* **2003**, *15*, 66–78.
- Labbé, R. F.; Vreman, H. J.; Stevenson, D. K. Zinc Protoporphyrin: A Metabolite with a Mission. *Clin. Chem.* **1999**, *45*, 2060–2072.
- Maliepaard, M.; Scheffer, G. L.; Faneye, I. F.; van Gastel, M. A.; Pijnenborg, A. C. L. M.; Schinkel, A. H.; van de Vijver, M. J.; Schepers, R. J.; Schellens, J. H. M. Subcellular localization and distribution of the breast cancer resistance protein transporter in normal human tissues. *Cancer Res.* **2001**, *61*, 3458–3464.
- Krishnamurthy, P.; Schuetz, J. D. Role of ABCG2/BCRP in biology and medicine. *Annu. Rev. Pharmacol. Toxicol.* **2006**, *46*, 381–410.
- Rosenbach-Belkin, V.; Chen, L.; Fiedor, L.; Tregub, I.; Pavlotsky, F.; Brumfeld, V.; Salomon, Y.; Scherz, A. Serine conjugates of chlorophyll and bacteriochlorophyll: Photocytotoxicity in vitro and tissue distribution in mice bearing melanoma tumors. *Photochem. Photobiol.* **1996**, *64*, 174–181.
- Mazor, O.; Brandis, A.; Plaks, V.; Neumark, E.; Rosenbach-Belkin, V.; Salomon, Y.; Scherz, A. WST11, a novel water-soluble bacteriochlorophyll derivative: cellular uptake, pharmacokinetics, biodistribution and vascular-targeted photodynamic activity using melanoma tumors as a model. *Photochem. Photobiol.* **2005**, *81*, 342–351.
- Schüller, J.; Cassidy, J.; Dumont, E.; Roos, B.; Durston, S.; Banken, L.; Utoh, M.; Mori, K.; Weidekamm, E.; Reigner, B. Preferential activation of capecitabine in tumor following oral administration to colorectal cancer patients. *Cancer Chemother. Pharmacol.* **2000**, *45*, 291–297.
- Bellnier, D. A.; Ho, Y.-K.; Pandey, R. K.; Misset, J. R.; Dougherty, T. J. Distribution and elimination of photofrin II in mice. *Photochem. Photobiol.* **1989**, *52*, 221–228.
- Omata, T.; Murata, N. Preparation of chlorophyll a, chlorophyll b, and bacteriochlorophyll a by column chromatography with DEAE-Sepharose CL-6B and Sepharose CL-6B. *Plant Cell Physiol.* **1983**, *24*, 1093–1100.
- Fiedor, L.; Rosenbach-Belkin, V.; Scherz, A. The stereospecific interaction between chlorophylls and chlorophyllase. Possible implication for chlorophyll biosynthesis and degradation. *J. Biol. Chem.* **1992**, *267*, 22043–22047.
- Schreck, R. Further quantitative methods for the study of transplantable tumors. The growth of R39 sarcoma and Brown–Pearce carcinomas. *Am. J. Cancer* **1936**, *28*, 345–363.
- Hyrc, K.; Wilczek, A.; Cieszka, K. Electrophoretic heterogeneity of pigmented melanoma cells. *Pigment Cell Res.* **1993**, *6*, 100–110.